Ecological Modelling 224 (2012) 76–89

Contents lists available at SciVerse ScienceDirect

Ecological Modelling

journal homepage: www.elsevier.com/locate/ecolmodel

Performance of a Bayesian state-space model of semelparous species for stock-recruitment data subject to measurement error

Zhenming Su[a,*], Randall M. Peterman[b]

[a] Institute for Fisheries Research, Michigan Department of Natural Resources, and University of Michigan, 212 Museums Annex Building, 1109 N. University Ave., Ann Arbor, MI 48109-1084, USA
[b] School of Resource and Environmental Management, Simon Fraser University, 8888 University Drive, Burnaby, B.C., V5A 1S6 Canada

ARTICLE INFO

Article history:
Received 25 January 2011
Received in revised form 26 October 2011
Accepted 1 November 2011
Available online 26 November 2011

Keywords:
Stock-recruitment analysis
Measurement error
Errors-in-variables
Time-series bias
State-space model
Bayesian
Markov chain Monte Carlo

ABSTRACT

Measurement errors in spawner abundance create problems for fish stock assessment scientists. To deal with measurement error, we develop a Bayesian state-space model for stock-recruitment data that contain measurement error in spawner abundance, process error in recruitment, and time series bias. Through extensive simulations across numerous scenarios, we compare the statistical performance of the Bayesian state-space model with that of standard regression for a traditional stock-recruitment model that only considers process error. Performance varies depending on the information content in data, as determined by stock productivity, types of harvest situations, and amount of measurement error. Overall, in terms of estimating optimal spawner abundance S_{MSY}, the Ricker density-dependence parameter β, and optimal harvest rate h_{MSY}, the Bayesian state-space model works best for informative data from low and variable harvest rate situations for high-productivity salmon stocks. The traditional stock-recruitment model (TSR) may be used for estimating α and h_{MSY} for low-productivity stocks from variable and high harvest rate situations. However, TSR can severely overestimate S_{MSY} when spawner abundance is measured with large error in low and variable harvest rate situations. We also found that there is substantial merit in using h_{MSY} (or benchmarks derived from it) instead of S_{MSY} as a management target.

1. Introduction

The relationship between spawning stock abundance (S) and subsequent recruitment (R) is fundamental for fish population dynamics (Quinn and Deriso, 1999). Parameter estimates for such relationships provide the basis for setting key values of variables used in fisheries management. However, traditional stock-recruitment analyses that use standard regression and treat S as an independent variable and R as a dependent variable are fraught with estimation problems (Hilborn and Walters, 1992). One major issue with these analyses is that they rarely consider error caused by mismeasuring S (measurement or observation error). However, mismeasurement of S is quite common in fisheries science (Hilborn and Walters, 1992; Needle, 2001). Analyses that ignore this error may be subject to severe bias in parameter estimates, which may result in serious management problems (Walters and Ludwig, 1981). Furthermore, large natural variation in survival rate from eggs to recruitment (McGurk, 1986) and dynamic feedbacks in stock-recruitment systems also exacerbate the difficulty of estimating stock-recruitment parameters (Hilborn and Walters, 1992).

To deal with the drawbacks of traditional stock-recruitment analysis, several researchers have developed other methods. One of them is an "errors-in-variables" (EV) approach (Ludwig and Walters, 1981; Schnute, 1994; Schnute and Kronlund, 2002). The EV method explicitly represents both natural variability and measurement errors inherent in the data. Unfortunately, the EV method requires that an assumption be made about what proportion of the total variation is due to measurement error; this step is necessary to avoid a model identification problem, i.e., a situation where model parameters cannot be uniquely estimated (Schnute, 1994). However, we rarely have data on that proportion, thus, many authors assume it is 0.5 (e.g., Ludwig and Walters, 1981). Nevertheless, there is little basis for this assumption, and this proportion's value can potentially greatly influence the resulting parameter estimates of the stock-recruitment function, as we show later.

Another more advanced method, state-space modeling (Harvey, 1989), has been applied to stock-recruitment analysis by several researchers, including Meyer and Millar (2001), Rivot et al. (2001), Schnute and Kronlund (2002), and Walters and Martell (2004). Here, we also used a state-space model applied to stock-recruitment data on Pacific salmon (*Oncorhynchus* spp.), but we went beyond what other authors have done by developing

* Corresponding author. Tel.: +1 734 663 3554.
E-mail addresses: suz@michigan.gov (Z. Su), peterman@sfu.ca (R.M. Peterman).

0304-3800/$ – see front matter © 2011 Published by Elsevier B.V.
doi:10.1016/j.ecolmodel.2011.11.001

a version of it that contains three sources of uncertainty, i.e., measurement error in spawning stock size, process stochasticity in recruitment, and the effect of time series bias. The latter bias arises due to non-random scatter of data points caused by linkage between a given year's recruitment anomaly and the subsequent spawner abundance (Walters, 1985). For the fitting process, we develop a Bayesian approach via Markov chain Monte Carlo (MCMC) sampling to make inferences about the state-space model (Clark, 2007). The Bayesian approach is the most general method for fitting non-linear state-space models (Millar and Meyer, 2000), whereas other methods, such as the EV and extended Kalman filter methods (Schnute and Kronlund, 2002), have more limitations (Rivot et al., 2004).

Compared to our model, Walters and Martell (2004) considered the effects of time series bias and process error in recruitment, but they did not consider measurement error in spawner abundance. The state-space models of Meyer and Millar (2001) and Schnute and Kronlund (2002) are most similar to ours, but they were formulated only for a cohort (i.e., a single reproductive line) of a salmon population. Thus, their models cannot be readily applied to the more usual situation in which data sets on spawners and recruits arise from multiple cohorts from the same population, which must be modeled simultaneously (e.g., there are 4 successive cohorts of fish for Fraser River sockeye salmon (*Oncorhynchus nerka*), because most of them mature at age 4, reproduce, and then die). Rivot et al. (2001) considered both process error in recruitment and measurement error in spawner abundance in their state-space models, but they assumed that recruitment did not affect the subsequent spawning stock and thus ignored possible effects of time series bias. Our state-space model includes harvesting and the full time-dynamic life cycle with feedback between recruitment and subsequent spawner abundance, which thereby considers time series bias in the data we are fitting.

The state-space modeling framework proposed in this paper can be valuable for fish stock-recruitment analysis and management. Often, the only available data for stock-recruitment analysis are a single time series of estimates of the number of spawners and recruits. Even in this case, the cost for collecting these data is often high. Thus, it will be cost-effective if the state-space modeling approach can provide improved estimates of parameters over the traditional ones, especially because such parameters affect management decisions (Walters and Martell, 2004).

State-space modeling has been increasingly used in ecological applications to quantify multiple sources of uncertainty (Peterman et al., 2000; Harwood and Stokes, 2003; Buckland et al., 2004; Rivot et al., 2004). However, due to their complexity, state-space models are computationally very intensive and difficult to fit (de Valpine and Hastings, 2002; Clark, 2007). Thus, most of these models, including the ones that we investigate, have not yet been subject to extensive evaluation by means of simulations across wide ranges of scenarios/situations to determine their performance relative to that of simpler standard regression models that only consider one source of uncertainty (Walters and Martell, 2004).

This study is an attempt to fill this gap by using simulations to assess the performance of a state-space model that explicitly incorporates measurement error and to compare it to the performance of a traditional stock-recruitment model that ignores measurement error. We intend to examine the impact of measurement error in spawning stock size (S) on both models under a wide range of situations, and identify situations where the consequences of mismeasuring S are substantial and thus remedies for that impact are essential. For this purpose, we used simulations to generate numerous data sets with varying information content and uncertainty in the data about the estimated parameters, as determined by combinations of six factors: age at maturity, productivity parameter values, harvest situations, amount of measurement error, autocorrelation in time series of annual recruitments due to environmental effects, and number of data points.

We compare performance of these two models, the traditional and state-space versions of the Ricker model (Quinn and Deriso, 1999), in terms of bias, precision of parameter estimates, and accuracy of estimates of uncertainty (Adkison and Su, 2001; Browne and Draper, 2006). The statistical properties of model parameters and other derived quantities used for setting management targets are relevant for conservation and management of fisheries resources (Quinn and Deriso, 1999). To cope with the large computational burden of our extensive simulations, we developed a customized MCMC sampling program for this study.

2. Methods

2.1. Models

2.1.1. Salmon population dynamics, fishing, and management

In this simulation study, we use two Pacific salmon species, pink salmon (*Oncorhynchus gorbuscha*) and sockeye salmon, as case examples to examine the effect of measurement error in spawner abundance on stock-recruitment analysis. Because adults of Pacific salmon all die after spawning (i.e., semelparous) and there is no overlap of individuals between generations, their dynamics can be described by relationships that connect the number of spawners and recruits between two generations (Quinn and Deriso, 1999).

Fishing for salmon occurs on homeward-migrating adult returns (recruits) in coastal waters, and salmon management is mainly concerned with managing fisheries so as to allow an adequate number of returning fish to escape the fisheries to spawn (escapement). Thus, data for salmon management mainly come from catch and escapement records. The number of spawners is usually determined from estimates of spawners on the spawning grounds, which can be subject to errors due to counting methods and procedures, observers, and physical conditions (Cousens et al., 1982; Su et al., 2001). Catch is obtained from fishing reporting systems and stock-identification methods in mixed-stock fisheries, and is usually more accurately estimated than the number of spawners (Quinn and Deriso, 1999).

Pacific salmon exhibit a wide range of life histories (Groot and Margolis, 1991). Whereas pink salmon go to sea directly as fry and invariably mature and return two years after spawning, other salmon species have various lengths of freshwater and marine residence, leading to variable age at maturity (Larkin, 1988). To simplify our analysis, we only consider the constant single-age-at-maturity situation.

2.1.2. The state-space Ricker stock-recruitment model (SSR)

As already noted, parameter estimates obtained from traditional stock-recruitment analysis (defined in Section 2.1.3) that ignores errors in estimates of spawner abundance may be misleading (Walters and Ludwig, 1981). To attempt to overcome this problem, we use state-space modeling (Harvey, 1989). State-space models are time series models featuring observed variables as well as unobserved states. The state-space spawner-recruit model (SSR) proposed here uses an observation equation to incorporate the effects of error caused by mismeasuring spawner abundance and a system equation that deals with process uncertainty caused by environmental factors on recruitment. We utilize the state-space model to track the population dynamics of a salmon population with a constant age at maturity of k (Fig. 1).

First, the unobserved true number of spawners S_t at year t is related to the measured number of spawners (escapement) E_t by an observation equation, where t is a relative year index with $t = 1$ referring to the first year of data collection. As is traditional (Walters

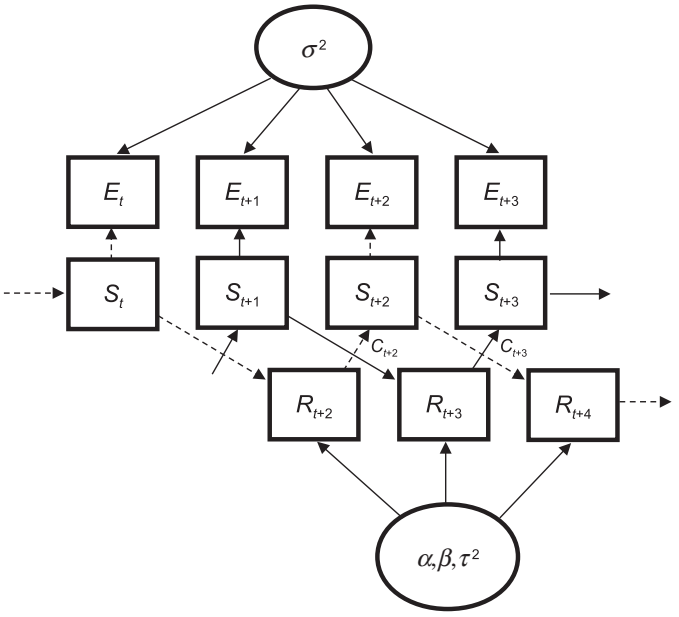

Fig. 1. Illustration of the population dynamics of an example pink salmon population with a constant age at maturity of 2 years. Dashed lines connect quantities for years t, $t+2$, $t+4$, etc., and solid lines connect quantities for years $t+1$, $t+3$, etc. These even- and odd-year lines (cohorts) of pink salmon thus have separate population dynamics and are reproductively isolated. E_t is the measured number of spawners, S_t is the unobserved true number of spawners, R_t is the unobserved true number of recruits, and C_t is the catch. Greek symbols refer to estimated parameters of the state-space Ricker stock-recruitment model, as defined later in the text.

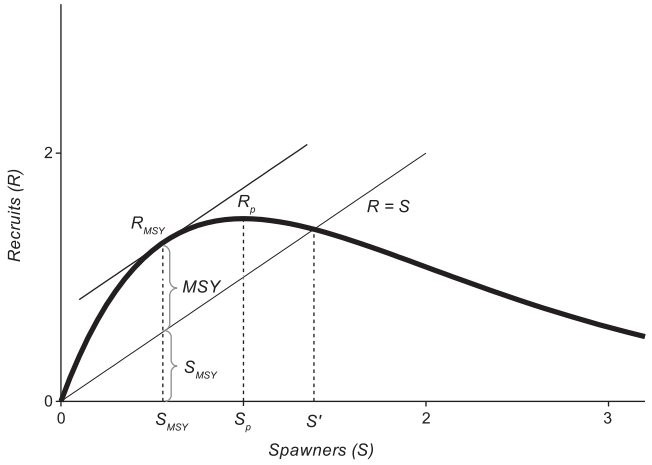

Fig. 2. The Ricker spawner (S)–recruit (R) curve and related management-oriented quantities in arbitrary units. $R=S$ along the diagonal replacement line, hence S' = unfished equilibrium abundance of R and S, i.e., carrying capacity. Maximum sustainable yield or catch (MSY) occurs at S_{MSY}, the spawner abundance at which there is the maximum vertical distance between R and the replacement line, indicated by the tangent to the curve (thin solid straight line) at R_{MSY}. Peak recruitment (R_p) occurs at spawner abundance $S_p = 1/\beta$.

and Martell, 2004), we assume a log-normal probability distribution for E_t:

$$E_t = S_t \exp(v_t), \quad t = 1, \ldots, T \tag{1a}$$

where $v_t \overset{iid}{\sim} N(0, \sigma^2)$ and denotes measurement error, σ^2 is the measurement error variance, and T is the last year in the data set.

Second, we use two system equations to describe the transitions of spawners and recruitment between two generations of the same cohort of a salmon population. The first equation defines a stochastic stock-to-recruitment process that relates the true spawners S_{t-k} (where k is age at maturity in years) to the true recruitment R_t produced by S_{t-k}. This is the Ricker stock-recruitment function (Quinn and Deriso, 1999; see Fig. 2):

$$R_t = \alpha S_{t-k} \exp(-\beta S_{t-k} + w_{t-k}), \quad t = k+1, \ldots, T \tag{1b}$$

where α is a productivity parameter reflecting the number of recruits per spawner at low spawner abundance (slope at the origin), β measures the strength of density-dependence and describes how quickly the recruits-per-spawner decrease as spawning stock increases, $w_t \overset{iid}{\sim} N(0, \tau^2)$ is process error, and τ^2 is the process-error variance. The initial state variables are S_1 to S_k for the k cohorts. The error terms v_t and w_t are assumed to be uncorrelated.

The second system equation defines the transition from the recruitment R_t at t to the spawners S_t in the presence of fishing, which occurs only on returning fish (R_t) before they spawn. As noted above, catch from many salmon fisheries is usually relatively well-measured compared to escapement (Quinn and Deriso, 1999), so we assume that catch, C_t, is measured without error. In this case, S_t is then:

$$S_t = R_t - C_t \tag{1c}$$

Parameters of this state-space model (Eqs. (1a)–(1c)) are $\boldsymbol{\theta} = \{\alpha, \beta, \sigma^2, \tau^2, S_1, \ldots, S_k\}$. This state-space model is illustrated in Fig. 1.

It is more convenient to work with an additive normal error structure, so we take the natural logarithms of both sides of Eqs. (1a)–(1c) and let $y_t = \log_e(E_t)$, $x_t = \log_e(S_t)$, $r_t = \log_e(R_t)$, and $a_r = \log_e(\alpha)$, thus transforming Eqs. (1a)–(1c) to the following:

$$y_t = x_t + v_t, \quad t = 1, \ldots, T \tag{2a}$$

$$r_t = a_r + x_{t-k} - \beta \exp(x_{t-k}) + w_{t-k}, \quad t = k+1, \ldots, T \tag{2b}$$

$$x_t = \log_e(\exp(r_t) - C_t) \tag{2c}$$

Parameters of the state-space model in Eq. (2) are $\boldsymbol{\theta} = \{a_r, \beta, \sigma^2, \tau^2, x_1, \ldots, x_k\}$ and data are $\boldsymbol{Y} = \{y_t, C_t\}$. Here C_t is a control variable and its values are treated as fixed constants used to update x_t. We define the state vector as $\boldsymbol{r} = \{r_{k+1}, \ldots, r_T\}$. In Eq. (2b), r_t implicitly depends on r_{t-k} through Eqs. (2b) and (2c), and the transition of r_t from r_{t-k} follows a first-order Markov process.

2.1.3. Traditional Ricker stock-recruitment model (TSR)

Most traditional stock-recruitment analyses assume that spawning stock size S is measured without error, i.e., $\sigma^2 = 0$ in Eq. (1a). In this case, only process error in recruitment enters the analysis. Based on this assumption, the traditional stock-recruitment model (TSR) is defined as:

$$R_t^{obs} = \alpha E_{t-k} \exp(-\beta E_{t-k} + \varepsilon_{t-k}), \quad t = k+1, \ldots, T \tag{3}$$

where the measured number of recruits $R_t^{obs} = E_t + C_t$, $\varepsilon_t \sim N(0, \sigma_\varepsilon^2)$ is model error, and σ_ε^2 is the model error variance. Dividing both sides of Eq. (3) with E_{t-k} and taking logarithms yields:

$$\log_e\left(\frac{R_t^{obs}}{E_{t-k}}\right) = a_r - \beta E_{t-k} + \varepsilon_{t-k}, \quad t = k+1, \ldots, T \tag{4}$$

This is a simple linear regression model of $\log_e(R_t^{obs}/E_{t-k})$ on E_{t-k}. Given pairs of data $\{E_{t-k}, R_t^{obs}\}$, standard regression techniques are often used to obtain parameter estimates for this model (Hilborn and Walters, 1992).

There are two potential estimation problems with Eq. (4). First, using the error-prone E_{t-k} rather than the true and error-free S_{t-k} as an independent variable (X) violates one important assumption of standard regression (no measurement error in the X variable), and that may lead to biased estimates of parameters (Hilborn and Walters, 1992). Second, due to the nature of dynamic stock-recruitment systems, spawning stock size is not a controlled

independent variable (unlike what standard regression assumes), but instead is stochastic because it is generated by previous recruitment, which is also a random variable. This can cause what Walters (1985, 1990) called time series bias in parameter estimates.

Biases caused by both measurement error and the time series effect often co-exist in stock-recruitment data for fishes and are inseparable, so both sources of bias should be considered simultaneously (Caputi, 1988). Traditional stock-recruitment (TSR) analysis does not do this, whereas a state-space stock-recruitment (SSR) analysis does. Here, we compare the performance of these two approaches.

2.1.4. Deterministic relationships and management-oriented quantities

Management of most Pacific salmon fisheries is based on quantities derived from two deterministic relationships between stock and recruitment at equilibrium conditions: $R = \alpha S \exp(-\beta S)$ and $S = R - C$. The spawning stock size (S_{MSY}) that produces a maximum sustainable yield (catch) (MSY) can be found as the solution to the equation: $(1-\beta S)\alpha \exp(-\beta S) = 1$ (Fig. 2). Recruitment at MSY is then $R_{MSY} = \alpha S_{MSY} \exp(-\beta S_{MSY})$ and $MSY = R_{MSY} - S_{MSY}$ (Fig. 2). Harvest rate at MSY (h_{MSY}) is obtained by $h_{MSY} = MSY/R_{MSY}$. To simplify calculations, Hilborn and Walters (1992) provide the following good approximations to h_{MSY} and S_{MSY} respectively in the range of $0 < a_r < 3$:

$$h_{MSY} \approx a_r(0.5 - 0.07a_r) \tag{5a}$$

$$S_{MSY} \approx \frac{a_r(0.5 - 0.07a_r)}{\beta} \tag{5b}$$

We use these two equations to calculate h_{MSY} and S_{MSY} from the estimates of a_r and β, and evaluate their statistical properties along with those for other model parameters.

Other quantities we use are the unfished spawning stock size (carrying capacity) $S' = \log_e(\alpha)/\beta$, peak recruitment $R_p = \alpha/(\beta \exp(1))$, and spawning stock size at peak recruitment $S_p = 1/\beta$ (Quinn and Deriso, 1999; see Fig. 2).

2.2. Parameter estimation by Bayesian methods

2.2.1. Estimation for the state-space model

Bayesian inferential methods for the state-space model (Eqs. (2a)–(2c)) are based on the posterior distribution of parameters $\boldsymbol{\theta}$ and states $\boldsymbol{r}$ given the data $\boldsymbol{Y}$, $p(\boldsymbol{\theta}, \boldsymbol{r}|\boldsymbol{Y})$ (Clark, 2007). To make inferences for $\boldsymbol{\theta}$, one needs to construct a marginal posterior distribution of $\boldsymbol{\theta}$ by integrating out the states $\boldsymbol{r}$ in $p(\boldsymbol{\theta}, \boldsymbol{r}|\boldsymbol{Y})$, i.e., $p(\boldsymbol{\theta}|\boldsymbol{Y}) = \int_r p(\boldsymbol{\theta}, \boldsymbol{r}|\boldsymbol{Y})\, d\boldsymbol{r}$ (Schnute, 1994). However, it is difficult to evaluate $p(\boldsymbol{\theta}|\boldsymbol{Y})$ directly by integration. MCMC simulation techniques bypass the need to evaluate the high dimensional integral in $p(\boldsymbol{\theta}|\boldsymbol{Y})$ by generating dependent draws from the posterior distribution $p(\boldsymbol{\theta}, \mathrm{r}|\boldsymbol{Y})$ via Markov chains (Gelman et al., 2004). From these simulated values, posterior summaries or the marginal posterior distributions of any parameters (or functions of the parameters) can be evaluated by simply using the simulation draws for these parameters.

To derive the joint posterior distribution $p(\boldsymbol{\theta}, \boldsymbol{r}|\boldsymbol{Y})$ for MCMC sampling, first we observe that $p(\boldsymbol{\theta}, \boldsymbol{r}|\boldsymbol{Y}) \propto p(\boldsymbol{\theta}, \boldsymbol{r})p(\boldsymbol{Y}|\boldsymbol{\theta}, \boldsymbol{r})$ based on Bayes' theorem (Gelman et al., 2004), where $p(\boldsymbol{Y}|\boldsymbol{\theta}, \boldsymbol{r})$ is the likelihood of the data given the states and the parameters, and $p(\boldsymbol{\theta}, \boldsymbol{r})$ is the joint prior distribution of $\boldsymbol{\theta}$ and $\boldsymbol{r}$. Based on the conditional independence assumption made for y_t (Eq. (2a)), the likelihood is given by

$$p(\boldsymbol{Y}|\boldsymbol{\theta}, \boldsymbol{r}) = \prod_{t=1}^{T} N(y_t|x_t, \sigma^2) \tag{6}$$

The prior $p(\boldsymbol{\theta}, \boldsymbol{r})$ can be further factored into the product of the prior distribution of the parameters, $p(\boldsymbol{\theta})$, and the hierarchical prior distribution of the states given $\boldsymbol{\theta}$, $p(\boldsymbol{r}|\boldsymbol{\theta})$. Based on the Markov property of the system equation (Eq. (2b)) $p(r_t|x_i, \ldots, x_{t-2k}, x_{t-k}) = p(r_t|x_{t-k})$, where x_i is one of $\{x_1, \ldots, x_k\}$, the joint prior distribution of the states $\boldsymbol{r}$ given $\boldsymbol{\theta}$, $p(\boldsymbol{r}|\boldsymbol{\theta}) = p(\{r_{k+1}, ..., r_T\}|\boldsymbol{\theta})$, can be derived as (Petris et al., 2009):

$$\begin{aligned} & p(\boldsymbol{r}|\boldsymbol{\theta}) \\ &= p(r_{k+1}|x_1, \boldsymbol{\theta})p(r_{k+2}|x_2, \boldsymbol{\theta}) \ldots p(r_T|x_i, \ldots, x_{T-2k}, x_{T-k}, \boldsymbol{\theta}) \\ &= p(r_{k+1}|x_1, \boldsymbol{\theta})p(r_{k+2}|x_2, \boldsymbol{\theta}) \ldots p(r_T|x_{T-k}, \boldsymbol{\theta}) \\ &= \prod_{t=k+1}^{T} N(r_t|a_r + x_{t-k} - \beta \exp(x_{t-k}), \tau^2) \end{aligned} \tag{7}$$

Substituting Eqs. (6) and (7) into $p(\boldsymbol{\theta}, \boldsymbol{r}|\boldsymbol{Y})$, we obtain the joint posterior distribution $p(\boldsymbol{\theta}, \boldsymbol{r}|\boldsymbol{Y})$ as:

$$\begin{aligned} & p(\boldsymbol{\theta}, \boldsymbol{r}|\boldsymbol{Y}) \propto p(\boldsymbol{\theta})p(\boldsymbol{r}|\boldsymbol{\theta})p(\boldsymbol{Y}|\boldsymbol{\theta}, \boldsymbol{r}) \\ &= p(\boldsymbol{\theta}) \prod_{t=k+1}^{T} N(r_t|a_r + x_{t-k} - \beta \exp(x_{t-k}), \tau^2) \prod_{t=1}^{T} N(y_t|x_t, \sigma^2) \end{aligned} \tag{8}$$

To perform Bayesian estimation, we need to specify prior distributions for the parameters $\boldsymbol{\theta}$. First, we assume that the initial state variables $x_t, t = 1, \ldots, k$, follow a normal distribution, $N(m_0, V_0)$, with $m_0 = 0$ and $V_0 = 10^3$. Because x_t values are in a log scale, these priors are very diffuse. We assign uniform prior distributions for the Ricker $a_r = \log_e(\alpha)$ and β parameters (Millar, 2002): $a_r \sim U(0, \infty)$ and $\beta \sim U(0, \infty)$. We also assign uniform priors for σ and τ: $\sigma \sim U(0, \infty)$ and $\tau \sim U(0, \infty)$ (Gelman and Hill, 2007) because the often-used non-informative prior $p(\tau^2) \propto 1/\tau^2$ or inverse gamma distribution $IG(\varepsilon, \varepsilon)$ with small ε can create problems for hierarchical prior variance parameters (such as τ^2) with values near zero (Gelman and Hill, 2007).

We estimate model parameters and states for the state-space model (Eq. (2)) by sampling from the posterior distribution in Eq. (8) using a Markov chain Monte Carlo method (MCMC) (Gelman et al., 2004). Although WinBUGS (Lunn et al., 2000) can be used to make inferences for our state-space model, it is not feasible to use it for this extensive simulation study because of the large computational burden for the nearly 20,000 simulated datasets we examined. To overcome this computational problem, we developed our own MCMC sampling program based on the full conditional distributions derived from the posterior distribution (Eq. (8)). In Appendix A, we provide two full conditional distributions, one for updating the vector (a_r, β) in a block, and the other for updating the individual recruitment r_t. The full conditional distributions of the other parameters can be derived easily and are available from the first author.

2.2.2. Estimation for the traditional Ricker stock-recruitment model

For the traditional Ricker model (Eq. (4)), we have the following posterior distribution:

$$p(\boldsymbol{\theta}|\boldsymbol{Y}) \propto p(\boldsymbol{\theta}) \prod_{t=k+1}^{T} N(\log_e(R_t^{obs})|a_r + \log_e(E_{t-k}) - \beta E_{t-k}, \sigma_\varepsilon^2) \tag{9}$$

where $\boldsymbol{\theta} = \{a_r, \beta, \sigma_\varepsilon^2\}$. As for the SSR model, we assume $a_r \sim U(0, \infty)$ and $\beta \sim U(0, \infty)$, and $\sigma_\varepsilon \sim U(0, \infty)$. We use a MCMC sampler to update a_r and β by a bivariate normal conditional distribution similar to Eq. (A1) and σ_ε^2 by an inverse-gamma conditional distribution.

2.3. Simulation analyses

2.3.1. The simulation model

We simulate escapement, recruitment, and catch data for a hypothetical Pacific salmon stock with a constant age at maturity k. We generate each simulated data set in two phases. In phase 1, the initialization phase, starting from $t = -25k$, we set S_t to the unfished carry capacity $R' = S' = \log_e(\alpha^*)/\beta^*$ for the first k years. Here we use an asterisk to denote parameters used in the simulation model to differentiate them from the parameters used in the estimation model (Eq. (1) or (2)). Then we sequentially generate new recruits (R_{t+k}), catch (C_{t+k}), and spawners (S_{t+k}) up to $t = k$ by

$$\begin{aligned} R_{t+k} &= \alpha^* S_t \exp(-\beta^* S_t + w_t) \\ w_t &= \lambda w_{t-1} + u_t,\ u_t \sim N(0, \tau^{*2}) \\ C_{t+k} &= h_{t+k} R_{t+k} \\ S_{t+k} &= R_{t+k} - C_{t+k} \end{aligned} \tag{10}$$

where h_t is set to a constant initial harvest rate h_1, which we specify in Section 2.3.2. To allow for possible autocorrelated environmental effects on recruitment, we assume that w_t follows a first-order autoregressive process (AR(1)), and denote λ as the autocorrelation coefficient. At the end of phase 1, we obtain realized values of S_1 to S_k and keep them as the initial state values for phase 2. Other values from this phase are discarded. The initial states thus generated are random and depend on the historical fishing level h_1 (which we explore later with different values), thus addressing the related concerns of Kope (1988).

In phase 2, the data generation phase, starting from $t = 1$ and using the realized values of S_1 to S_k, we generate R_{t+k}, C_{t+k}, and S_{t+k} using Eq. (10) up to $t = T - k$. More details for h_t are given in Section 2.3.2. We also calculate $E_t = S_t \exp(v_t)$ with $v_t \sim N(0, \sigma^{*2})$ for $t = 1, \ldots, T$. Finally, $\{E_t\}_{t=1}^{T}$ and $\{C_t\}_{t=k+1}^{T}$ are kept as the data used for each simulation.

Because we use time-dynamic models to produce the simulated data to which we apply the two estimation models, time series bias implicitly contributes to the resulting estimation errors, along with measurement and process errors.

2.3.2. Simulation scenarios

We consider a wide range of conditions for six factors that may affect performance of our two models: (1) values of the true Ricker α parameter: α^*; (2) types of harvest situations; (3) proportion of the total error variance ($V = \sigma^{*2} + \tau^{*2}$) that is due to measurement error: $\rho^* = \sigma^{*2}/V$; (4) values of age at maturity, k; (5) values of the autocorrelation coefficient in process errors, λ; and (6) number of data points in the time series, T. The true parameter values considered in the simulations are listed in Table 1. Each simulation scenario corresponds to one combination of these six sets of conditions.

We consider three types of harvest situations in our simulations. First, we generate harvest rates that vary over time using a piecewise linear equation:

$$h_t = \begin{cases} h_1 + (h_2 - h_1)(t-k)/(0.5T), & k+1 \le t \le k+0.5T \\ h_2 + (h_1 - h_2)(t-k-0.5T)/(0.5T), & k+0.5T < t \le T \end{cases} \tag{11}$$

for $t = k+1, \ldots, T$, where h_1 is the initial harvest rate used in phase 1 of the simulation model (Eq. (10)), and h_2 is a maximum harvest rate. We set $h_1 = 0.2h_{MSY}$, and $h_2 = 1.0h_{MSY}$, and refer to this harvest situation as "variable harvests", where h_{MSY} is the true harvest rate at *MSY*. This harvest situation produces a relatively high-contrast fishing history, which corresponds to a fishery starting data collection when exploitation is very low ($0.2h_{MSY}$), then with a harvest rate that increases linearly to $1.0h_{MSY}$ at $t = k + 0.5T$, and decreases to a small value at the end of the fishing history. The stock-recruitment data generated by this harvest situation contain data points for both high and low spawner abundance, thus providing information for potentially estimating α and β reasonably well.

Table 1
True values used for parameters in the simulation model. The notes provide more explanations for these values. θ stands for "parameter".

θ	Values	Notes
α^*	2, 4, 8	These values correspond to the 10th percentile, median, and 90th percentile of α values obtained from data on 43 pink salmon stocks by Su et al. (2004).
β^*	1	β determines the absolute level of population size, as shown by the unfished equilibrium carrying capacity $S' = \log_e(\alpha)/\beta$. Different populations have different abundance levels, but we can always scale their abundance to a unit that makes the magnitude of β one. Therefore, in the simulations, we set the true value of β to one. This produces populations with size near one unit of fish, e.g., one unit might be 10^4 fish for a Pacific salmon population.
τ^{*2}	0.5	A relatively large process error variance
σ^{*2}	0.0, 0.17, 0.5, 1.5	$\sigma^{*2} = 0$ is used to test the independent effects of time series bias on parameter estimates in the absence of measurement error.
ρ^*	0, 0.25, 0.5, 0.75	$\rho^* = \sigma^{*2}/(\sigma^{*2} + \tau^{*2})$
k	2, 4	$k = 2$ and 4 are used to simulate pink and sockeye salmon, respectively.
λ	0, 0.5	The first-order autocorrelation coefficient
T	16, 28, 60	Number of data points

We also generate two fixed-harvest rate situations using harvest rates of $0.2h_{MSY}$ or $1.15h_{MSY}$, which we denote as "low harvests" and "high harvests", respectively. The low harvest situation results in a fishery that starts its data collection when exploitation is low and this low harvest rate continues through time, i.e., $h_t = 0.2 \times h_{MSY}$, for $t = -25k$ to T. The stock-recruitment data generated by this harvest situation contain data points at both low and high spawning abundance, thus providing information for estimating β as well as α (Fig. 3a and b). In contrast, the high harvest situation with $h_t = 1.15 \times h_{MSY}$ for $t = -25k$ to T results in a fishery starting data collection with a highly exploited population and with persistent high harvest rates through time. The stock-recruitment data generated by this harvest situation only contain data points at low spawning abundance, thus providing little information for estimating β (Fig. 3c and d). All three situations have many real-world analogues for a variety of fish species.

We determine statistical properties of the two estimation methods across Monte Carlo simulations over a broad range of scenarios represented by numerous combinations of these six factors. Of these scenarios, 36 are composed of combinations of three levels of α^*, three types of harvest situations, and four levels of ρ^* for $k = 2$, $\tau^{*2} = 0.5$, $\lambda = 0$, and $T = 28$ (Table 1). We treat these 36 simulations as our baseline scenarios. In numerous sensitivity analyses, we evaluate the effect on baseline performance measures of age at maturity (k), autocorrelation in recruitment (λ), and number years of data T.

2.3.3. Performance measures

For each simulation scenario, we generate 300 sets of catch and escapement data using the simulation model (enough to produce stable performance metrics based on trials). For each data set, we run the two estimation models, SSR and TSR, separately and obtain posterior median ($\tilde{\theta}$), 2.5th ($\theta_{2.5}$), 25th (θ_{25}), 75th (θ_{75}), and 97.5th ($\theta_{97.5}$) percentiles from the posterior distribution of each parameter (θ) from the MCMC sampling draws. For each of the 300 simulation runs of each scenario for a model, we record whether

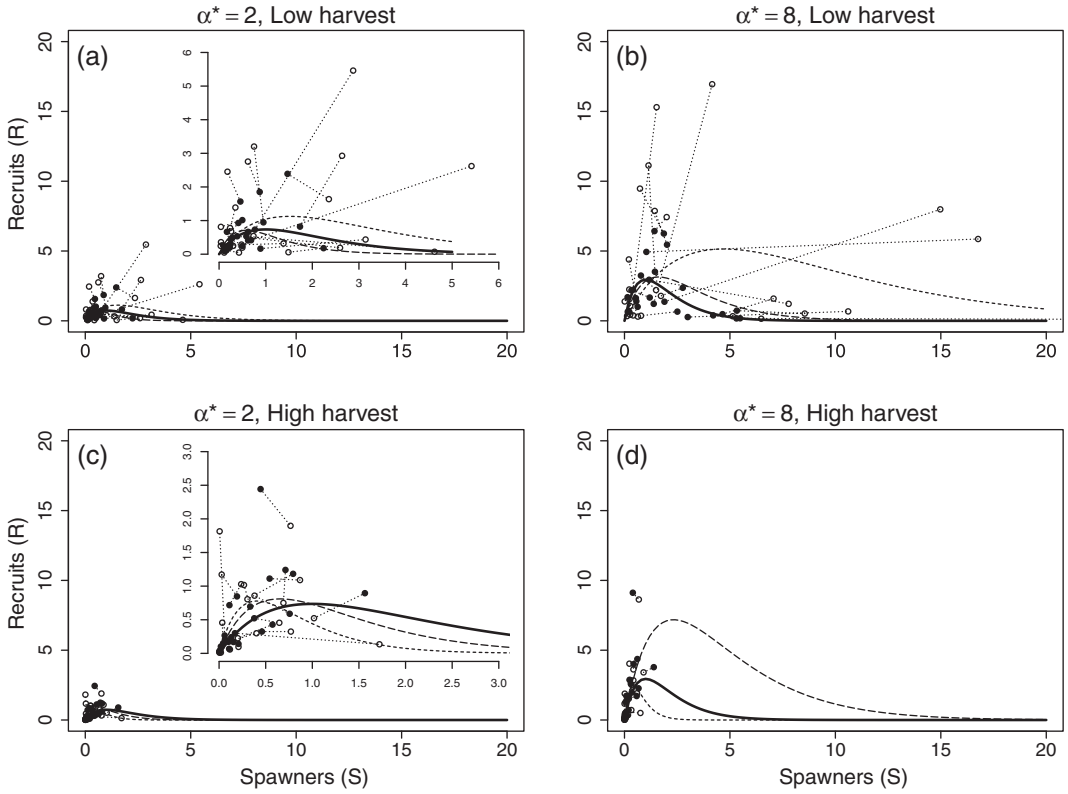

Fig. 3. Examples of single Monte Carlo runs of the simulation model that generated four simulated stock-recruitment data sets for combinations of two levels of α^* (true Ricker α parameter) and two types of harvest situations (fractions of h_{MSY}, "Low" = $0.2h_{MSY}$ and "High" = $1.15h_{MSY}$), given that $\tau^{*2} = 0.5$, $\rho^* = 0.75$, $\lambda = 0$, and $T = 28$ for stocks with age at maturity at 2. Solid dots represent true spawner and recruit points. Open circles represent observed data points. A dotted straight line indicates displacement of an observed point from a true point. A thick solid curved line represents the true stock-recruitment curve. A long-dashed curved line represents the stock-recruitment curve estimated from the state-space Ricker model (SSR). A dashed curved line represents the stock-recruitment curve estimated from the traditional Ricker stock-recruitment model (TSR). Inset graphs in panels (a) and (c) are close-ups of lower-left corners of those panels.

a 95% posterior interval ($\theta_{2.5}$, $\theta_{97.5}$) contained the true parameter value (θ^*), and calculate the percentage relative bias (*RB*) of the posterior median of each parameter compared to its true value as $RB = 100(\tilde{\theta} - \theta^*)/\theta^*$. We also calculate the coefficient of quartile variation (*CQV*) using $(\theta_{75} - \theta_{25})/(\theta_{75} + \theta_{25})$ to quantify uncertainty in parameter estimates. These two quantities, posterior median and *CQV*, are robust to outliers.

To summarize results for an estimation model across the 300 simulated data sets of a scenario, we calculate the median and interquartile range (*IQR*, or the difference between the 25th and 75th percentiles of a distribution) from the empirical distribution of the 300 *RB*s, and median of 300 *CQV*s for each parameter. We also calculate the actual coverage probability of a 95% probability interval from SSR and TSR as the percentage of intervals that contain the true parameter values. Because of the increasing importance in recent years of taking into account estimates of uncertainties in parameters and observed state variables related to conservation risks, such a coverage probability is an extremely important, yet infrequently used performance measure for evaluating parameter estimation methods (Adkison and Su, 2001). For instance, if the width of the probability distribution of a quantity is either under- or over-estimated, this will then bias calculations of risk in a stock assessment.

2.3.4. Preliminary results and MCMC sampling algorithm verification

First, we evaluated the implementation of our MCMC sampler for the Bayesian state-space model (SSR) by comparing its parameter estimates with those obtained from a WinBUGS program (Appendix B) for 20 data sets from the low or high harvest situation with $k = 2$, $\alpha^* = 4$, $\tau^{*2} = 0.5$, $\rho^* = 0.25$, $\lambda = 0$, and $T = 28$. They produced almost identical results (Table 2).

For our MCMC samplers, we conducted extensive pilot runs before the simulations to determine by means of MCMC diagnostic tests (Gelman et al., 2004) appropriate MCMC sampling details such as the total number of iterations (N), the length of burn-in period (B), and the thinning interval. Detailed descriptions of the diagnostics are given in Appendix C. Based on these diagnostics, we used $N = 1.5$ million, $B = 0.5$ million, and a thinning interval of 100 for all our calculations for the state-space model. In contrast, for TSR, we used $N = 0.43$ million, $B = 30{,}000$, and a thinning interval of 50. We also provided the results for a sensitivity analysis of different prior specifications for τ^2 and σ^2 in Appendix D.

Table 2
Averages of 20 posterior median values for each of four parameters from the Bayesian state-space model (SSR) or the WinBUGS program (BUGS) for $k = 2$, $\alpha^* = 4$, $\tau^{*2} = 0.5$, $\rho^* = 0.25$, $\lambda = 0$, $T = 28$, and the low or high harvest situation. θ stands for "parameter".

θ	Low		High	
	SSR	BUGS	SSR	BUGS
α	4.67	4.66	5.26	5.27
β	1.06	1.06	1.23	1.24
τ^2	0.42	0.41	0.32	0.32
σ^2	0.24	0.24	0.80	0.80

3. Results

3.1. Influence of stock productivity, harvest situations, and amount of measurement error

For our 36 baseline results, given true values of age at maturity $k = 2$, process error variance $\tau^{*2} = 0.5$, first order autocorrelation coefficient $\lambda = 0$, and the number of years $T = 28$, we compare parameter estimates of the two models (traditional Ricker model and the state-space version of it) based on three performance measures for four model parameters (α, β, σ, and τ) and two derived management parameters (S_{MSY} and h_{MSY}).

3.1.1. Bias in α, β, S_{MSY}, and h_{MSY}

First, in the absence of measurement error ($\rho^* = 0$), there is little bias in parameter estimates in most cases except for estimates of β and S_{MSY} with the high harvest rate situation at $\alpha^* = 2$ or 8 (Fig. 4). These latter cases reflect the effects of time series bias.

Measurement error in observed spawner abundance can cause biased parameter estimates for both the Bayesian state-space (SSR) and traditional Ricker stock-recruitment (TSR) models (Fig. 4). Although a moderate amount of measurement error ($\rho^* \leq 0.25$) may not induce much bias in most scenarios, a large amount can cause substantial bias in many situations (Fig. 4). The impacts of measurement error vary widely depending on stock productivity α^*, historical harvest patterns, amount of measurement error as indicated by ρ^*, models considered, and parameters examined, so we categorize results into various cases of these conditions and highlight key results below.

Stock productivity α^* and historical harvest patterns have a substantial effect on both the sign and magnitude of the bias, whereas the amount of measurement error mainly affects the magnitude of bias in estimates of all four estimated quantities, α, β, S_{MSY}, and h_{MSY} (Fig. 4). First, SSR overestimates α for low-productivity stocks ($\alpha^* \leq 4$) (Fig. 4a–f, first row). This bias increases with decreasing α^*, increasing ρ^*, and increasing average harvest rates. As a result, α is severely overestimated by SSR with larger values of ρ^* (>0.5) at $\alpha^* = 2$ with all three harvest situations (Fig. 4a–c). In contrast, in those same situations, TSR produces much less (but still positively) biased estimates of α than SSR at large values of ρ^* at $\alpha^* = 2$ (Fig. 4a–c) or at $\alpha^* = 4$ with the variable or high harvest situation (Fig. 4e and f). In other cases, estimates of α from TSR are either more negatively biased (Fig. 4d, g and h) or more positively biased (Fig. 4i) than those produced by SSR.

SSR overestimates β by a large amount at large values of ρ^* at $\alpha^* = 2$ (Fig. 4a–c, second row), produces just slightly biased

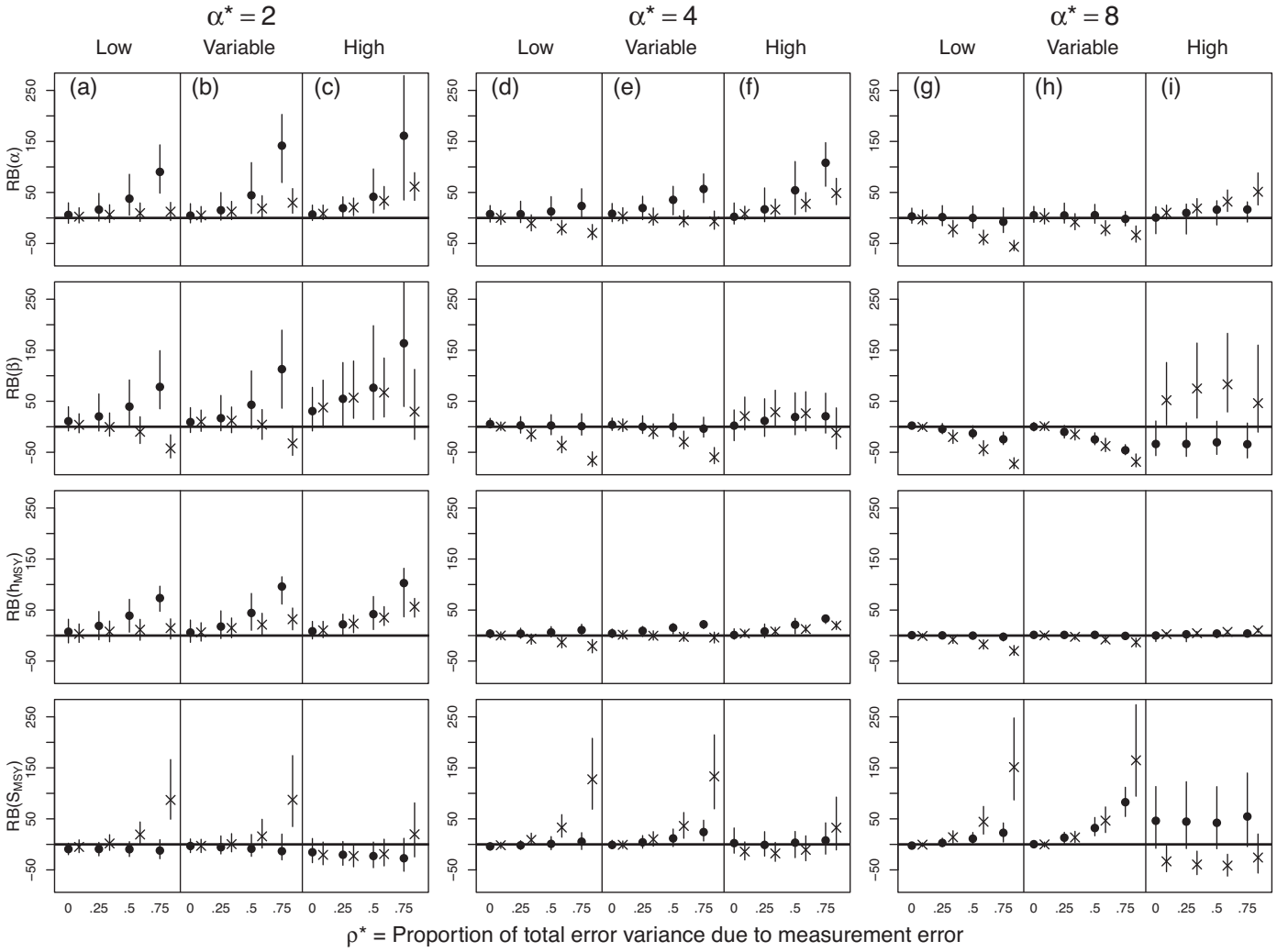

Fig. 4. Interquartile range (*IQR*: 25th to 75th percentiles, shown as vertical lines) and medians (symbols on lines) of 300 estimates of percentage relative biases (*RB*s) in estimates of four parameters of two models, i.e., α, β, h_{MSY}, and S_{MSY} (one parameter in each row, respectively, from top to bottom). Results are shown for $k = 2$, $\tau^{*2} = 0.5$, $\lambda = 0$, and $T = 28$, and different combinations of α^* (2, 4, 8), harvest situations (Low, Variable, and High), and ρ^* (0, 0.25, 0.5, 0.75). Models are indicated by solid dots = Bayesian state-space model (SSR), "X" = traditional Ricker model (TSR). The SSR methods have some $RB(\beta)$ values >270% in the second row of the vertical panel (c).

Table 3
Medians of 300 estimates of percentage relative biases (*RB*s) for σ and τ from the Bayesian state-space model for $k=2$, $\tau^{*2}=0.5$, $\lambda=0$, and $T=28$, and different combinations of α^* (2, 4, 8), harvest situations (Low, Variable, High), and ρ^* (0.25, 0.5, 0.75). Values greater than |40|% are highlighted with boldface.

Harvest situation	ρ^*	$\alpha^*=2$		$\alpha^*=4$		$\alpha^*=8$	
		σ	τ	σ	τ	σ	τ
Low	0.25	28	−17	23	−12	4	0
	0.5	13	−26	16	−25	3	−3
	0.75	5	**−46**	9	**−49**	8	−26
Variable	0.25	4	−5	26	−10	18	−6
	0.5	12	−10	23	−25	23	−15
	0.75	9	**−49**	16	**−54**	28	**−44**
High	0.25	−3	−2	**93**	−21	**492**	**−61**
	0.5	7	−4	**75**	−39	**273**	**−66**
	0.75	18	**−46**	**54**	**−61**	**146**	**−68**

estimates of β at $\alpha^*=4$ (Fig. 4d–f), but underestimates β (Fig. 4g–i) at $\alpha^*=8$. With the low and variable harvest situations at each value of α^*, TSR mostly underestimates β at large values of ρ^*, and the magnitude of underestimation increases with increasing α^* and ρ^* (Fig. 4a–b, d–e, and g–h, second row). This leads to more negatively biased estimates of β from TSR than those from SSR at larger values of ρ^* at $\alpha^*=4$ or 8 (Fig. 4d–e and g–h). With the high harvest situation, TSR tends to overestimate β, and in this case, the bias in β estimates is largest at intermediate levels of ρ^* (Fig. 4c, f and i).

The pattern of bias of estimates of h_{MSY} across scenarios (Fig. 4, third row) is very similar to that of α. However, the relative biases (*RB*s) of h_{MSY} are much smaller than those of α. Additionally, despite the large bias in the estimates of h_{MSY} from both SSR and TSR when $\rho^*>0.25$ at $\alpha^*=2$, bias of the h_{MSY} estimates from both models is very slight at $\alpha^*=4$ or 8 (Fig. 4).

The magnitude of *RB*s of S_{MSY} from SSR (Fig. 4, fourth row) is also much smaller than that of α and β. $RB(S_{MSY})$ from SSR is small and not sensitive to ρ^* except for cases at $\alpha^*=8$ with variable (for $\rho^*=0.75$, Fig. 4h) and high (for all levels of ρ^*, Fig. 4i) harvest rates. Compared to SSR, TSR can severely overestimate S_{MSY} at larger values of $\rho^*(0.75)$ with the low and variable harvest situations (Fig. 4a–b, d–e and g–h). TSR also causes highly negatively biased estimates of S_{MSY} at $\alpha^*=8$ with the high harvest situation at all levels of ρ^* (Fig. 4i).

As noted above, at $\alpha^*=8$ with the high harvest situation (Fig. 4i), both models have difficulties with estimating β and S_{MSY} because the data contain little information on β at all levels of ρ^* (Fig. 3d). TSR overestimates β by about 45–85% and underestimates S_{MSY} by about −25% to −42%. In contrast, SSR underestimates β by −32% but overestimates S_{MSY} by about 40–55%.

3.1.2. Bias in σ and τ

SSR tends to overestimate σ but underestimate τ, and estimates of τ become more negatively biased with the increase of ρ^* (Table 3). With the low and variable harvest situations for all α^* and the high harvest situation at $\alpha^*=2$, SSR produces estimates of σ and τ with relatively small bias (except for τ with $\rho^*=0.75$) (Table 3). However, SSR severely overestimates σ at $\alpha^*=4$ or 8 and underestimates τ at $\alpha^*=8$ with the high harvest situation (Table 3).

3.1.3. Measures of uncertainty

Coefficients of quartile variation (*CQV*s) from SSR are usually larger than those from TSR, but SSR produces close to nominal 95% coverage probability more often than TSR (Table 4b). The coverage probability of TSR is especially poor for S_{MSY} at $\alpha^*=4$ and 8 and when $\rho^*\geq 0.5$ with the low or variable harvest situation. High harvest rates also lead to deteriorated coverage probability for both models when $\rho^*\geq 0.5$ (Table 4b).

3.2. Influence of age at maturity k and autocorrelation

Both k and λ have little effect on relative bias of parameter estimates for h_{MSY} and S_{MSY} for both SSR and TSR (Table 5, compare *RB*s for different k (or λ) at the same λ (or k) and ρ^* for the same model). Analogous effects of k and λ are found on *RB* of other parameters (results not shown).

3.3. Influence of the number of data points T

Increasing the number of data points (T) leads to less biased estimates (for $\alpha^*=2$ and 4) or no change (for $\alpha^*=8$) in the estimates of α, β, h_{MSY}, and S_{MSY} of SSR, but leads to more biased estimates of S_{MSY} at all α^* and α, β, h_{MSY} at $\alpha^*=4$ and 8 for TSR (Table 6).

3.4. Using known ρ in the estimation of SSR

As observed in Section 3.1, SSR has difficulties with fitting data from the high harvest situation, especially at $\alpha^*=8$. For these data, we evaluate whether fixing ρ to 0.5 (i.e., assuming that half the total variance is due to measurement error) can ease the problem. Compared to our baseline case where ρ is a free parameter, SSR with $\rho=0.5$ has a substantial effect on estimates of β and S_{MSY} at $\alpha^*=8$ with the high harvest situation (Table 7). This case reverses the sign of bias for the estimates of β and S_{MSY}. At $\alpha^*=2$ and $\rho^*=0.75$, fixed ρ reduces the bias in the estimates of α, β, and h_{MSY} substantially.

4. Discussion

4.1. Conclusions

This paper makes three new contributions to the analysis of one of the most fundamental relationships in modeling of fish population dynamics, the stock-recruitment relationship. First, we extended previous Bayesian state-space stock-recruitment models for salmon populations (Meyer and Millar, 2001; Schnute and Kronlund, 2002) to take into account both measurement error and process variation together in a time-dynamic model that generated time-series bias as well. We also developed full Bayesian estimation procedures and a computer program for this nonlinear state-space model. Second, by evaluating our Bayesian state-space stock-recruitment model across broad ranges of simulation conditions, we contributed to the understanding of nonlinear state-space models that consider multiple sources of uncertainty, in particular the effects of measurement error. Third, we provided new insights into the effects of measurement error on the traditional stock-recruitment models under combinations of conditions not considered previously.

From our results, we found that measurement error in spawning stock size might lead to bias in parameter estimates for both the Bayesian state-space Ricker stock-recruitment model (SSR) and the traditional Ricker stock-recruitment model (TSR). In addition, performance of the two models varies considerably with harvest situations, stock productivity, and amount of measurement error in data. All three of these factors can alter the information content about parameters in the data, as discussed in Sections 4.2 and 4.3 below, thereby affecting the performance of the models at estimating those parameters. Increasing the number of data points may be beneficial to the state-space model but may lead to more biased parameter estimates for the traditional Ricker model. On the other hand, age at maturity and autocorrelation are less influential to the estimates.

To summarize the results, we divide our data into two types based on information contrast in spawner abundance (S) as determined by stock productivity and harvest situations. First is a

Table 4
(a) Medians of 300 coefficients of quartile variation (*CQV*s), and (b) Actual coverage probability of 95% intervals (*CVRG*) for h_{MSY} and S_{MSY}, under α^* (2, 4, 8), ρ^* (0, 0.5, 0.75), and three harvest situations (Low, Variable, High), with $k = 2$, $\tau^{*2} = 0.5$, $\lambda = 0$, and $T = 28$. Models are: SSR: Bayesian state-space model; TSR: traditional Ricker stock-recruitment model. θ stands for "parameter".

Harvest	θ	Model	$\alpha^*=2$			$\alpha^*=4$			$\alpha^*=8$			Average
			0	0.5	0.75	0	0.5	0.75	0	0.5	0.75	
(a) CQV (%)												
Low	h_{MSY}	SSR	23	25	24	9	15	17	4	7	10	15
		TSR	19	22	27	8	14	21	4	11	20	16
	S_{MSY}	SSR	15	19	24	8	15	21	5	13	19	15
		TSR	13	17	24	6	11	19	4	10	19	14
Variable	h_{MSY}	SSR	20	22	19	9	11	12	4	6	8	12
		TSR	18	19	21	8	11	13	4	7	10	12
	S_{MSY}	SSR	16	20	22	11	16	19	7	16	20	16
		TSR	15	16	20	8	11	15	5	9	14	13
High	h_{MSY}	SSR	16	16	15	9	10	8	8	8	7	11
		TSR	15	15	16	7	7	7	3	3	4	9
	S_{MSY}	SSR	25	23	23	26	23	22	28	25	25	24
		TSR	22	18	19	21	15	16	30	20	18	20
		Average	18	19	21	11	13	16	9	11	14	15
(b) *CVRG* (%): values ≤85% are highlighted in boldface												
Low	h_{MSY}	SSR	97	96	92	98	99	99	97	99	99	97
		TSR	98	98	98	97	88	92	97	**72**	**65**	89
	S_{MSY}	SSR	98	96	97	100	99	99	98	96	96	98
		TSR	97	97	93	96	**83**	**68**	94	**58**	**48**	**82**
Variable	h_{MSY}	SSR	94	86	**71**	94	96	96	95	97	99	92
		TSR	93	92	93	95	96	98	92	88	86	93
	S_{MSY}	SSR	98	97	96	99	93	88	99	**78**	**38**	87
		TSR	96	90	**74**	96	**56**	**18**	94	**29**	**8**	**62**
High	h_{MSY}	SSR	94	**74**	**54**	97	88	**78**	92	95	94	**85**
		TSR	95	**80**	**77**	95	**80**	**77**	94	**76**	**69**	**83**
	S_{MSY}	SSR	96	**82**	**78**	97	92	90	**81**	**75**	**60**	**83**
		TSR	95	**81**	**72**	96	**77**	**49**	93	**70**	**60**	**77**
		Average	96	89	**83**	97	87	**79**	94	**78**	**69**	**86**

Table 5
Medians of 300 estimates of percentage relative biases (*RB*s) of h_{MSY} and S_{MSY} from the Bayesian state-space (SSR) and the traditional Ricker stock-recruitment (TSR) models for two levels of age at maturity k (2, 4), two levels of first-order autocorrelation coefficients ($\lambda = 0$ or 0.5), and four levels of ρ^* (0, 0.25, 0.5, 0.75) with $\alpha^* = 4$, $\tau^{*2} = 0.5$, $T = 28$, and the variable harvest history. θ stands for "parameter".

θ	Model	k	$\lambda = 0$				$\lambda = 0.5$			
			$\rho^*=0.0$	$\rho^*=0.25$	$\rho^*=0.5$	$\rho^*=0.75$	$\rho^*=0.0$	$\rho^*=0.25$	$\rho^*=0.5$	$\rho^*=0.75$
h_{MSY}	SSR	2	4	9	16	22	1	3	11	22
		4	5	6	11	21	6	7	12	21
	TSR	2	2	0	−3	−4	−2	−4	−4	−4
		4	2	−1	−3	−2	2	1	−1	0
S_{MSY}	SSR	2	−1	4	12	24	2	6	14	22
		4	−1	7	17	28	−1	6	16	32
	TSR	2	−1	10	36	133	2	9	30	119
		4	−2	9	30	110	−3	6	29	109

low-information type that exhibits low contrast in S, including data sets at a productivity of $\alpha^* = 2$ with all harvest situations and at $\alpha^* = 4$ or 8 with high harvest rates. Second is a high-information type that has high contrast in S, including data sets generated by low or variable harvest rates at $\alpha^* = 4$ or 8. Overall, the Bayesian state-space model (SSR) works best for informative data sets. With the low or variable harvest situation, it is the best performer in terms of estimating S_{MSY} (for all α^*), β (for $\alpha^* = 4$ or 8), and α and h_{MSY} (for $\alpha^* = 8$) with the smallest relative bias, and it gives the most accurate estimate of uncertainty in parameter estimates (i.e., 95% coverage probabilities). For data sets with poor information (e.g., $\alpha^* = 2$), the simpler model, TSR, often outperforms SSR in terms of estimating

Table 6
Medians of 300 estimates of percentage relative biases (*RB*s) in four estimated parameters from the Bayesian state-space model (SSR) and the traditional Ricker stock-recruitment model (TSR), for three levels of the number of data points (T), with $\alpha^* = (2, 4, 8)$, $k = 2$, $\rho^* = 0.5$, $\lambda = 0$, and the "variable" harvest situation.

Model	θ	$\alpha^*=2$			$\alpha^*=4$			$\alpha^*=8$		
		$T=16$	$T=28$	$T=60$	$T=16$	$T=28$	$T=60$	$T=16$	$T=28$	$T=60$
SSR	α	72	45	16	38	36	22	5	6	2
	β	75	43	17	6	1	−3	−24	−25	−25
	h_{MSY}	63	44	19	16	16	10	1	2	1
	S_{MSY}	−13	−8	2	7	12	13	33	32	34
TSR	α	32	19	11	0	−5	−10	−18	−22	−30
	β	22	4	−5	−20	−30	−35	−33	−38	−44
	h_{MSY}	34	21	14	0	−3	−6	−6	−8	−12
	S_{MSY}	2	16	23	20	36	42	34	46	56

Table 7
Median of 300 estimates of percentage relative biases (*RBs*) of estimated parameters (θ) from the Bayesian state-space model with ρ as an estimated parameter (*free*) and the same model except with ρ fixed to 0.5 (*fixed*), for $k = 2$, $\tau^{*2} = 0.5$, $\lambda = 0$, $T = 28$, and different combinations of α^* (2, 8) and ρ^* (0.25, 0.75) with the high harvest situation.

θ	ρ	$\alpha^* = 2$		$\alpha^* = 8$	
		$\rho^* = 0.25$	$\rho^* = 0.75$	$\rho^* = 0.25$	$\rho^* = 0.75$
α	Fixed	18	64	−5	24
	Free	19	161	10	17
β	Fixed	47	95	25	45
	Free	55	164	−34	−34
h_{MSY}	Fixed	20	58	−1	6
	Free	22	103	3	4
S_{MSY}	Fixed	−15	−18	−18	−27
	Free	−20	−27	45	55

α and h_{MSY}. However, TSR can severely overestimate S_{MSY} when S is measured with large error in low and variable harvest situations.

4.2. Stock productivity, harvest situation, and contrast in spawner abundance

Broadly speaking, the performance of the two models is determined by the information about the model parameters that is contained in the data (Adkison, 2009), which is a function of the magnitude of measurement error and variation in spawner abundance, S. This general point is well known for traditional spawner-recruit analysis (Hilborn and Walters, 1992). The variation in S is in turn influenced by stock productivity (α) and harvest rates, as shown in Fig. 3. In the absence of harvesting, a spawning stock of a salmon population varies around its unfished carrying capacity $S' = \log_e(\alpha)/\beta$ based on the Ricker model. Therefore, for a given β, the range of S increases with increasing α value. On the other hand, a high harvest rate has the effect of restricting the range of S. The combined effect of α and harvesting is to restrict S of low-productivity stocks ($\alpha^* = 2$) to very low values even at the low harvest situation (Fig. 3a). Similarly, the range of S from highly exploited stocks ($1.15h_{MSY}$) is also severely restricted to low spawning abundance, even at large values of α^* (Fig. 3d). In contrast, a wide range of S, including high spawner abundance, is produced by high-productivity stocks with a low (Fig. 3b) or variable exploitation rate.

The effects of contrast in S are apparent in our results. In our analyses of stocks with low productivity ($\alpha^* = 2$), contrast in S is low, and parameter estimates for α, β, and h_{MSY} have the largest estimation biases compared to scenarios with higher productivity. As well, for a given α^*, estimation bias is the largest with the high harvest situation, and coverage probabilities are the most underestimated. Therefore, scenarios with high harvest rates produced the worst performance measures.

Although the important influence of contrast in spawner abundance is very well known (Hilborn and Walters, 1992), the contribution to that contrast of different α values has not been explored thoroughly, even though it clearly influences how much S can change over time. For instance, Kehler et al. (2002) explored the effect of different α, but only for the standard estimation method for the basic Ricker model (our TSR). Our results for TSR regarding effects of the range of S on estimates of α are consistent with theirs, but they concluded that the underlying true α is not an important factor, unlike our study. The reason for these different conclusions is that the simulation model of Kehler et al. (2002) differs from ours. They first generated S based on uniform distributions and then generated R according to the Ricker model. This static method ignores possible time-series effects that we simulated here with our time-dynamic model. Thus, we conclude that the magnitude of bias due to measurement error is influenced by true productivity (α^*).

4.3. Effects of measurement error

We can understand the effects of measurement error in spawner abundance (S) on parameter estimates for both models by examining how measurement error affects the scatter of the observed stock/recruitment (SR) points relative to those of the true data points (Fig. 3). Measurement error has the effect of displacing observed data points (E_t, R^{obs}_{t+k}) from corresponding true points (S_t, R_{t+k}) both horizontally and vertically (Fig. 3) (Schnute and Kronlund, 2002). The direction and magnitude of such a displacement depend on where the true data point falls relative to the stock size at the peak recruitment $S_p = 1/\beta$ (Kehler et al., 2002). A true data point with $S < S_p$ tends to be displaced more vertically, whereas a true data point with $S > S_p$ tends to be displaced more horizontally (Kehler et al., 2002). The overall effect of measurement error will thus be influenced by where the bulk of true data points is located relative to S_p on the x-axis, which is in turn affected by harvest rates and true α value, as described in the previous section.

Lightly exploited stocks have more data points with $S > S_p$ (Fig. 3a and b) than heavily exploited stocks (Fig. 3c and d). For these data, measurement error has a larger chance of producing data points with large horizontal and vertical displacements and tends to spread the true SR points right- and upward (Fig. 3a and b). This produces observed SR points that appear to have lower initial slope (α) and lower density-dependent effect (β) values than the true SR points. In contrast, for spawning stocks that mainly fall below S_p, such as those with the high harvest rates, measurement error tends to shift the true SR points left and upward, producing observed SR points that appear to have larger initial slope (α) and larger β values than the true SR points (Fig. 3c and d).

The change in observed scatter caused by measurement error can have a direct impact on the parameter estimates of TSR because TSR tries to fit the observed recruitment data directly (Eq. (9)). For stocks subject to low harvest rates (Fig. 3a and b), observed SR points can greatly shift the fitted SR curve of TSR toward the right, causing large underestimates of α and β. On the other hand, for stocks subject to very high exploitation, TSR tries to fit the narrow range of observed data and overestimates α and β (Fig. 3d).

Unlike TSR, SSR takes measurement error into account in the parameter estimation (Schnute and Kronlund, 2002). Thus, for informative data, as from $\alpha^* = 8$ with the low harvest situation, the fitted SR curve from SSR is closer to the true curve than that of TSR, and SSR improves parameter estimates in this case over TSR (Fig. 3b).

The effects of measurement error on the traditional Ricker model have been investigated via simulation by several early studies (e.g., Walters and Ludwig, 1981; Caputi, 1988). However, those studies only explored a limited range of scenarios compared to our analyses. For instance, Walters and Ludwig (1981) only tested a single value of $\alpha^* = 2.72$. They found that TSR overestimated α, β, and h_{MSY}, but underestimated S_{MSY} for stocks subject to widely different initial exploitation rates in a closed-loop simulation. Although these biases are observed in some of our results for similar scenarios ($\alpha^* = 2$), we found, for productive stocks with $\alpha^* = 4$ or 8, that TSR is more likely to produce *negatively* biased estimates of α, β, and h_{MSY}, and positively biased estimates of S_{MSY} when harvest rates are either persistently low or widely variable.

4.4. Management implications

Our results also contribute useful new insights for discussions about the relative merits of management targets based on optimal escapement, S_{MSY}, compared to targets based on optimal percent

harvest rate, h_{MSY} (Walters and Martell, 2004). Theoretically, aiming to achieve S_{MSY} will produce the largest sustainable catch over the long term. However, in practice, S_{MSY}, which is a function of α and $1/\beta$, is frequently difficult to estimate with confidence due to large errors in estimating spawner abundance and poor estimates of β due to insufficient data at high S. Furthermore, due to practical difficulties of fine-tuning harvesting in small increments, S_{MSY} is difficult to achieve even if it were known perfectly. These disadvantages of S_{MSY} also apply to more biologically conservative targets that are some multiple of S_{MSY}. Walters and Martell (2004, p. 59) note the advantages of managing on the basis of setting a harvest rate such as h_{MSY} rather than setting a fixed escapement goal, S_{MSY}. The harvest rate, h_{MSY}, is only a function of the Ricker α parameter and fishing effort can be turned off and on in space and time such that a maximum percentage of fish can be caught by only allowing fishing for a limited time per week (Su and Adkison, 2002).

Our findings suggest that there is substantial merit in considering moving toward using h_{MSY} (or benchmarks derived from it) instead of S_{MSY} as a management target. For moderately to highly productive stocks with $\alpha^* = 4$ or 8, h_{MSY} is more reliably estimated *by both models* than S_{MSY}, as indicated by its smaller relative bias and its much narrower interquartile range across simulated data sets. As well, 95% coverage probabilities for h_{MSY} are closer to 95% for the widely used TSR method than S_{MSY}. Bias in estimates of h_{MSY} decreases rapidly with increasing α^*, and it is negligible at $\alpha^* = 8$ with variable or high harvest rates. However, in our low-productivity case with $\alpha^* = 2$, S_{MSY} is generally estimated better than h_{MSY} based on relative bias; at $\alpha^* = 2$, SSR and TSR produce h_{MSY} estimates that are highly positively biased at larger values of ρ^*. Such large positive bias in h_{MSY} may lead to overexploitation of fish stocks and create severe conservation risks. The main options for managers in this case are to improve accuracy of spawner abundance measurement and/or reduce target harvest rates by some safety margin. Low-productivity stocks are also prone to being overfished in mixed-stock fisheries and are hard to rebuild (Quinn and Deriso, 1999). For all α^*, TSR always has smaller positive bias or larger negative bias in h_{MSY} than SSR, so is more biologically conservative than SSR. This implies that, for fisheries that use h_{MSY} as target, using TSR would lead to lower biological risk.

Nevertheless, most fisheries for pink, sockeye, and chum (*Oncorhynchus keta*) salmon currently have escapement goals based on S_{MSY} or a target derived from it (Quinn and Deriso, 1999; Su and Adkison, 2002), rather than being managed for a target based on h_{MSY}. For estimating S_{MSY}, we prefer the Bayesian state-space modeling approach to TSR. At large values of measurement error ρ^*, relative biases of S_{MSY} from the SSR model are much smaller than those from TSR with low and moderate harvest rates. However, at larger α^* and ρ^*, TSR and SSR tend to over-estimate S_{MSY}. Positive bias in S_{MSY} implies under-utilization of resources (leaving more spawners than necessary) and a biologically conservative management policy. This may be beneficial for fish populations but may lead to long-term foregone social and economic benefits from harvesting.

For fisheries scientists involved in recovery planning in a conservation situation where a population is currently depleted, it is critical to obtain good quality estimates of α to estimate both the maximum percentage harvest rate that could be tolerated, as well as the potential rate of recovery if the cause of depletion is removed. Similar to the previous case with h_{MSY}, the best method of data analysis depends on α^* and harvest histories. For lower productivity stocks ($\alpha^* = 2$ or 4), TSR is preferred. In contrast, for higher productivity stocks ($\alpha^* = 8$), SSR is preferred. However, if the emphasis is on obtaining good quality estimates of S_{MSY} for identifying what is called a lower limit reference point on spawner abundance (e.g., 10% of S_{MSY}), SSR should be used.

4.5. Other considerations and future research

To attempt to improve parameter estimates, it is possible to use prior information about the Ricker α parameter that is available in Su et al. (2004) for 43 pink salmon populations and in Mueter et al. (2002) for 40 chum and 37 sockeye populations. Although incorporation of such an informative prior distribution for α or other parameters could reduce the *overall average* bias for the two estimation methods considered, that step would create biased estimates of α for individual stocks with below- or above-average α due to the shrinkage effect of such estimators (Gauch, 2006).

Alternative prior specifications for β, or equivalently using different parameterizations for the Ricker model, may have a strong influence on the Bayesian estimation methods. The seemingly reasonable non-informative priors used for β in this study, or for h_{MSY} and S_{MSY} used by Schnute and Kronlund (2002), may bring potential unexpected information to one's analysis (Rivot et al., 2001). A key need for future research is to use habitat information as covariates to predict unfished carrying capacity ($\log_e(\alpha)/\beta$). Simulation tests with this approach for Skeena River salmon data indicate that it can greatly help to reduce biases in both h_{MSY} and S_{MSY} (Carl Walters, Fisheries Centre, 2202 Main Mall, University of British Columbia, Vancouver, B.C., Canada V6T 1Z4, personal communication).

Our state-space stock-recruitment model explicitly represents both measurement error in spawner abundance and process error in recruitment. It is an extension of the state-space model proposed by Walters and Martell (2004, pp. 167–173), which did not consider measurement error in spawner abundance. Both of these state-space models incorporate a stochastic stock-to-recruitment process and a deterministic recruitment-to-stock process. Therefore, both can deal with time series bias (Walters, 1985, 1990). However, Walters and Martell (2004, pp. 167–173) demonstrated that state-space models may be not helpful for correcting time series bias for individual stocks. Thus, the biases in parameter estimates observed in this study are partially due to time series bias as indicated by the bias in β and S_{MSY} estimates in some of the high harvest rate situations when $\rho^* = 0$. Time series bias may have a large effect on stocks with smaller α^*, few data points, and fixed harvest rates. However, this bias diminishes with increasing α^* and for variable harvest rates (Korman et al., 1995). Simulation analyses like ours need to be done to compare Walters' (1990) bias correction method with our results. Walters and Martell (2004) and Walters et al. (2008) develop and apply another possible solution to time series bias based on correlated variation across fish stocks. Specifically, their state-space models can reduce bias in α and β estimates for a set of stocks that have been subject to strong and shared environmental effects such as those found in pink, chum, and sockeye salmon in the Northeastern Pacific (Pyper et al., 2005).

In this paper, we assumed that catch is measured without error. Although that error is often relatively small compared to observation error on spawner abundance, some measurement error in catch undoubtedly exists in real fisheries. Scientists can incorporate this error into analyses by adding an observation equation for catch to the state-space model, as proposed by Meyer and Millar (2001). We expect similar or even greater difficulties in separately estimating three error variances, rather than just two as in our SSR method.

Acknowledgments

This study was funded partially by Federal Aid Project F-80 R-9 to the Michigan Department of Natural Resources, Study 230557 conducted by Zhenming Su at the Institute for Fisheries Research. Funding was also provided by a Strategic Projects grant to R.M. Peterman, C.C. Wood, M.J. Bradford, and D.M. Ware from the

Natural Sciences and Engineering Research Council of Canada, and the Canada Research Chairs Program to R.M. Peterman. We thank Milo Adkison, Rob Kronlund, Marc Mangel, Steve Martell, Terrance Quinn II, and Carl Walters for reviewing an earlier draft manuscript, and two anonymous reviewers for many helpful comments on this manuscript.

Appendix A. Full conditional distributions

A.1. Updating the vector $\boldsymbol{\varphi} = (a_r, \beta)'$

First we derive the full conditional distribution of the vector $\boldsymbol{\varphi} = (a_r, \beta)'$ by making use of the conditionally linear property of Ricker $a_r = \log(\alpha)$ and β (r_t is a linear function of a_r and β):

$$\text{Let } \boldsymbol{X} = \begin{pmatrix} 1 & -S_1 \\ \vdots & \vdots \\ 1 & -S_{T-k} \end{pmatrix}_{(T-k)\times 2}, \quad \boldsymbol{Y} = \begin{pmatrix} \log_e(R_{k+1}) - \log_e(S_1) \\ \vdots \\ \log_e(R_T) - \log_e(S_{T-k}) \end{pmatrix}_{(T-k)\times 1}$$

and based on the uniform prior distributions for a_r and β: $a_r \sim U(0,\infty)$ and $\beta \sim U(0,\infty)$, we obtain the following full conditional distribution of $\boldsymbol{\varphi}$, which is used to update a_r and β in a block:

$$p(\boldsymbol{\varphi}|\cdot) \propto N(\hat{\boldsymbol{\varphi}}, \hat{\boldsymbol{V}}) \tag{A1}$$

where $\hat{\boldsymbol{V}} = (\tau^{-2}(\boldsymbol{X}'\boldsymbol{X}))^{-1}$, $\quad \hat{\boldsymbol{\varphi}} = \hat{\boldsymbol{V}}(\tau^{-2}\boldsymbol{X}'\boldsymbol{Y})$.

A.2. Update state variable $r_t = \log_e(R_t)$ using an independence-chain algorithm

The conditional distribution of the state r_t is

$$p(r_t|r_{t-k}, r_{t+k}, \boldsymbol{\theta}, y_t) = p(r_t|r_{t-k}, a_r, \beta, \tau^2)p(r_{t+k}|r_t, a_r, \beta, \tau^2)p(y_t|x_t, \sigma^2) \tag{A2}$$

where $t = k+1, \ldots, T$.

Eq. (A2) is not a standard density function. Following Geweke and Tanizaki (2001), we use an independence-chain sampling algorithm to update r_t. In this algorithm, we take the density function of the system equation in Eq. (2b), as the proposal distribution of the Metropolis–Hastings algorithm (Geweke and Tanizaki, 2001):

$$q(r^*) = p(r^*|r_{t-k}^{(i)}) = N(r^*|a_r^{(i)} + x_{t-k}^{(i+1)} - \beta^{(i)}S_{t-k}^{(i+1)}, (\tau^2)^{(i)}) \tag{A3}$$

where i is the current iteration number of the sampler.

The proposal distribution $q(r^*)$ does not depend on the current value of r_t, $r_t^{(i)}$, therefore, it is called an independence-chain algorithm (Chib and Greenberg, 1995). The r_t can be updated using the general Metropolis–Hastings algorithm. To update each r_t, a candidate value r^* is drawn from Eq. (A3). Then r^* is accepted as an update for r_t with a probability:

$$\min\left(1, \frac{p(r_{t+k}^{(i)}|r^*)p(y_t|r^*)}{p(r_{t+k}^{(i)}|r_t^{(i)})p(y_t|r_t^{(i)})}\right) \tag{A4}$$

otherwise, we reject r^* and set $r_t^{(i+1)} = r_t^{(i)}$.

Appendix B. WinBUGS program for the state-space Ricker model

```
model
{
  # Observation equation
  for (t in 1:T)
  {
    E[t] ~ dlnorm(mu.logE[t], prec.E); mu.logE[t] <-
log(S[t]);
  }
  # Prior distributions for the state variables
  for (t in 1:k)
  {
    S[t] <- S1[t]; S1[t] ~ dlnorm(0.0, 1.0E-3)
  }
  for (t in 1:(T - k)) {
    mu[t] <- b[1] + log(S[t]) - b[2] * S[t];
    R[t] ~ dlnorm(mu[t], prec.R)I(C[t], 1.0E+9); # R and C
represent R_{t+k} and C_{t+k}, respectively
    S[t + k] <- R[t] - C[t];
  }
  # Prior distributions for model parameters
  # a bivariate normal prior for a_r and beta
  b[1:2] ~ dmnorm(mu.b[], prec[,])
  a_r <- b[1]; alpha <- exp(b[1]);
  beta <- b[2]
  # Priors for standard deviations
  tau ~ dunif(0, 1.0E+9); tau2 <- tau * tau; prec.R <-
1/tau2
  sig ~ dunif(0, 1.0E+9); sig2 <- sig * sig; prec.E <-
1/sig2
  # Management-oriented quantities
  SMSY <- hMSY/beta
  hMSY <- 0.5*a_r - 0.07*a_r *a_r
}
```

Note: This program uses a bivariate normal prior distribution for a_r and β. This instructs WinBUGS to update a_r and β in a block as was done for our Bayesian state-space model (SSR). However, a_r and β are not restricted to be positive as in the case for a_r and β in SSR. Nevertheless, the results from the WinBUGS program can be compared to those from SSR by discarding those draws with non-positive a_r and β.

Here is an example data set generated from the conditions: $k = 2$, $\alpha^* = 4$, $\beta^* = 1$, $\tau^{*2} = 0.01$, $\sigma^{*2} = 0.003$, $\rho^* = 0.25$, $\lambda = 0$, $T = 28$, and the "variable" harvest situation:

```
Data: list(mu.b = c(1, 1), prec = structure(.Data = c(1.0E-03,
0, 0, 1.0E-06), .Dim = c(2, 2)), T = 28, k = 2, E = c(1.062,
1.179, 1.385, 1.213, 1.176, 1.385, 1.141, 0.944, 1.087, 1.119,
0.966, 0.918, 0.793, 0.775, 0.645, 0.661, 0.548, 0.703, 0.807,
0.792, 0.9, 1.007, 1.222, 1.269, 1.001, 1.108, 1.032, 1.099),
C = c(0.165, 0.23, 0.272, 0.34, 0.385, 0.409, 0.508, 0.596,
0.609, 0.669, 0.674, 0.779, 0.708, 0.864, 0.611, 0.658, 0.631,
0.583, 0.548, 0.534, 0.556, 0.513, 0.332, 0.319, 0.235, 0.2))
Inits:
list(b = c(6, 2), tau = 2, sig = 3, R = c(1, 1, 1, 1, 1, 1, 1,
1, 1, 1, 1, 1, 1, 1, 1, 1, 1, 1, 1, 1, 1, 1, 1, 1, 1, 1), S1 =
c(1, 1))
list(b = c(3, 0.5), tau = 1, sig = 1, R = c(2, 2, 2, 2, 2, 2,
2, 2, 2, 2, 2, 2, 2, 2, 2, 2, 2, 2, 2, 2, 2, 2, 2, 2, 2, 2),
S1 = c(2, 2))
Results: posterior medians for (α,β,τ²,σ²) from WinBUGS are
(4.05,1.18,0.0071,0.0066) and those from our program are
(4.05,1.00,0.0075,0.0055).
```

Appendix C. MCMC diagnostics

To assess convergence of the MCMC simulation runs of the Bayesian state-space model (SSR) and the traditional Ricker model (TSR), we calculated detailed MCMC diagnostic statistics for 50 randomly selected data sets from the 300 data sets of each of 18 selected scenarios (Table A1). For each data set, we ran 3 chains with dispersed parameter starting values for a total number of $N = 0.8$ million (m) iterations, a thinning interval (*Thin*) of 80 iterations and stored all sampling draws. Using the R CODA

Table A1
Summaries of MCMC diagnostics over 50 data sets and three levels of $\alpha^* = (2, 4, 8)$ for four parameters from the Bayesian state-space model for $k = 2$, $\lambda = 0$, and $T = 28$, and different combinations of ρ^* (0, 0.75) and harvest situations (Low, Variable, High). *Lag 1* – Average of lag-1 autocorrelation function. *Gelman* (%) – Average of percent of data sets with the Gelman–Rubin's potential scale-reduction factor greater than 1.1. *Geweke* (%) – Average of percent of data sets with the Geweke's diagnostic out of (−2, 2). *HW Stat* (%) or *HW hw* (%) – Average of percent of data sets failed with the Heidelberger and Welch's stationarity test or half-width test.

Diagnostic	Harvest	$\rho^* = 0$				$\rho^* = 0.75$			
		a_r	β	σ	τ	a_r	β	σ	τ
Lag	Variable	0.1	0.2	0.6	0.2	0.3	0.4	0.3	0.4
1	Low	0.1	0.2	0.4	0.3	0.2	0.4	0.2	0.3
	High	0.3	0.2	0.6	0.3	0.4	0.5	0.3	0.4
Gelman	Variable	0	0	7	0	0	0	3	0
	Low	1	1	5	1	0	0	1	0
	High	1	1	3	0	0	0	0	0
Geweke	Variable	0	1	3	2	2	1	0	0
	Low	1	1	2	2	0	0	1	2
	High	1	1	4	1	1	1	2	2
HW	Variable	0	1	3	2	1	0	1	0
stat	Low	1	1	3	2	1	0	1	1
	High	2	2	3	2	2	8	1	1
HW	Variable	0	1	8	2	1	1	1	0
hw	Low	1	1	3	2	1	0	1	1
	High	2	4	5	3	1	1	1	1

package (Plummer et al., 2006), we calculated the autocorrelation function (*acf*), Gelman–Rubin's potential scale-reduction factor (*psrf*), Geweke's diagnostic, and Heidelberger and Welch's diagnostic. We also examined *psrf* plots (*gelman.plot*), which shows the evolution of *psrf*'s as a function of the number of iterations, to determine the burn-in period (the number of initial iterations discarded).

For the Bayesian state-space model (SSR), the *psrf* plots showed that α, β, h_{MSY}, and S_{MSY} converged quickly (mostly less than 10,000 iterations). However, the observation error standard deviation σ showed very slow mixing in its chains for a moderate number of data sets, especially for those generated with $\rho^* = 0$ (no measurement error) or small ρ^* (<0.5). The process error standard deviation τ converged more quickly than σ, but slower than other parameters. The diagnostic statistics in Table A1 show the same convergence issue of σ for some data sets with $\rho^* = 0$. However, other parameters at both $\rho^* = 0$ and 0.75 and σ at $\rho^* = 0.75$ show no convergence problem for majority (over 96%) of the data sets examined.

As a further examination, we compared summary statistics of parameter estimates for 8 data sets (Table A2) from three different MCMC simulation settings (*N*, *B*, *Thin*) for SSR: *Short* – (0.23 m, 0.03 m, 20), where "m" is millions, *Median* – (0.43 m, 0.03 m, 50), *Long* – (1.5 m, 0.5 m, 100), where *B* – number of initial iterations discarded (burn-in). These settings yield essentially the same results. Similar results are found for other summary statistics (the coefficient of quartile variation, coverage probability) and other data sets. This indicates that our results are stabilized even for the short-run setting (0.23 m, 0.03 m, 20). However, all our results for the state-space model are based on the long runs (1.5 m, 0.5 m, 100) to minimize any effects of these simulation settings.

Table A2
Medians of 300 estimates of percentage relative biases (*RB*s) for six parameters from the Bayesian state-space model for $k = 2$, $\lambda = 0$, and $T = 28$ and different combinations of α^* (2, 8), harvest situations (Low, High), and ρ^* (0, 0.75) with three different MCMC sampling settings (*N*, *B*, *Thin*): *Short* – (0.23 m, 0.03 m, 20), where "m" is million iterations, *Median* – (0.43 m, 0.03 m, 50), *Long* – (1.5 m, 0.5 m, 100), where *N* – total number of iterations, *B* – number of initial iterations discarded (burn-in), and *Thin* – thinning interval. *RB*s for σ at $\rho^* = 0$ are not calculated because the true value of σ is zero in this case.

α^*	Harvest	ρ^*	Setting	α	β	σ	τ	h_{MSY}	S_{MSY}
2	High	0	Short	7	31		−9	9	−15
			Median	7	31		−9	9	−15
			Long	7	31		−9	9	−15
		0.75	Short	159	165	16	−45	102	−28
			Median	159	167	18	−45	102	−28
			Long	161	164	18	−46	103	−27
	Variable	0	Short	4	9		−8	5	−3
			Median	4	9		−8	5	−3
			Long	5	9		−8	6	−3
		0.75	Short	142	111	9	−49	96	−13
			Median	142	111	9	−49	96	−13
			Long	142	113	9	−49	96	−13
8	High	0	Short	0	−34		−59	0	46
			Median	2	−35		−59	1	48
			Long	1	−34		−59	0	46
		0.75	Short	16	−36	146	−68	4	56
			Median	17	−35	146	−69	4	54
			Long	17	−34	146	−68	4	55
	Variable	0	Short	5	0		−5	1	1
			Median	5	0		−5	1	1
			Long	6	0		−5	2	0
		0.75	Short	−2	−45	28	−44	−1	81
			Median	−2	−45	28	−44	−1	81
			Long	−2	−46	28	−44	0	83

The traditional Ricker model (TSR) converges much more quickly than the state-space model (less than 10,000 iterations). The results for (TSR) are based on a setting: (*N*, *B*, *Thin*) = (0.43 m, 0.03 m, 50).

Appendix D. Sensitivity analysis of prior probability distributions

Estimates from the Bayesian state-space model (SSR), especially those of σ^2 and τ^2, are sensitive to prior specifications of σ^2 and τ^2. An inverse Gamma $IG(\varepsilon, \varepsilon)$ prior with $\varepsilon = 0.001$ used for τ^2 and a

Table A3
Medians of 300 estimates of percentage relative biases (*RB*s) for six parameters from the Bayesian state-space model for $k = 2$, $\alpha^* = 4$, $\lambda = 0$, $T = 28$ for the variable and high harvest situations, and $\rho^* = (0.25, 0.75)$, with the uniform prior ($U(0, \infty)$) for σ or τ, or the inverse Gamma prior ($IG(0.001, 0.001)$) for σ^2 or τ^2.

Harvest	ρ^*	τ^2 or τ	σ^2 or σ	α	β	τ^2	σ^2	S_{MSY}	h_{MSY}
Variable	0.25	IG	IG	19	2	−15	−20	4	9
		IG	U	26	5	−40	124	3	12
		U	U	20	0	−19	60	4	9
		U	IG	11	−2	−3	−52	4	6
	0.75	IG	IG	73	2	−93	41	20	26
		IG	U	73	2	−94	53	21	26
		U	U	53	−3	−79	31	23	21
		U	IG	56	−4	−73	20	24	22
High	0.25	IG	IG	16	15	−32	122	−4	8
		IG	U	24	11	−67	436	3	11
		U	U	17	12	−38	273	−1	8
		U	IG	16	16	−17	−5	−8	8
	0.75	IG	IG	133	29	−94	129	4	37
		IG	U	133	25	−95	157	7	37
		U	U	108	21	−85	136	8	33
		U	IG	106	23	−82	109	4	33

uniform prior used for $\sigma \sim U(0, \infty)$, denoted as ($\tau^2 \sim IG, \sigma \sim U$), leads to the most negatively biased estimates of τ^2 and most positively biased estimates of σ^2 among the four prior combinations of τ^2 or σ^2 under the same scenario (Table A3). This in turn produces the most positively biased estimates of α and h_{MSY}. ($\tau^2 \sim IG$, $\sigma^2 \sim IG$) has similar effects on parameter estimates as ($\tau^2 \sim IG$, $\sigma \sim U$) with $\rho^* = 0.75$. In contrast, ($\tau \sim U, \sigma^2 \sim IG$) often leads to negatively biased or the least positively biased estimates of σ^2, the least negatively biased estimates of τ^2, and the least positively biased estimates of α and h_{MSY}. The parameter estimates from ($\tau \sim U, \sigma \sim U$) are close to those from ($\tau \sim U$, $\sigma^2 \sim IG$) (Table A3). In all cases, high correlation between the estimates of σ^2 and τ^2 are observed.

Based on these results and other similar results not shown, we prefer ($\tau \sim U$, $\sigma \sim U$) and ($\tau \sim U$, $\sigma^2 \sim IG$). However, the current Bayesian literature for prior specifications warns against using $IG(\varepsilon, \varepsilon)$ as a default prior for hierarchical variance parameters, such as τ^2 (Gelman and Hill, 2007). The $IG(\varepsilon, \varepsilon)$ distribution function is sharply peaked near zero. When data provide little information for the variance parameters τ^2 or σ^2, this prior can strongly constrain the posterior estimates near zero as indicated by our results (negatively biased estimates of τ^2 or σ^2). Based on this consideration, we choose ($\tau \sim U, \sigma \sim U$) as our default prior specification, although this prior choice may give more conservative (more biased) results than ($\tau \sim U$, $\sigma^2 \sim IG$) in some scenarios.

References

Adkison, M.D., 2009. Drawbacks of complex models in frequentist and Bayesian approaches to natural resource management. Ecol. Appl. 19, 198–205.

Adkison, M.D., Su, Z., 2001. A comparison of salmon escapement estimates using a hierarchical Bayesian approach versus separate estimation of each year's return. Can. J. Fish. Aquat. Sci. 58, 1663–1671.

Browne, W.J., Draper, D., 2006. A comparison of Bayesian and likelihood-based methods for fitting multilevel models. Bayesian Anal. 1, 473–550.

Buckland, S.T., Newman, K.B., Thomas, L., Koesters, N.B., 2004. State-space models for the dynamics of wild animal populations. Ecol. Model. 171, 157–175.

Caputi, N., 1988. Factors affecting the time series bias in stock-recruitment relationships and the interaction between time series and measurement error bias. Can. J. Fish. Aquat. Sci. 45, 178–184.

Chib, S., Greenberg, E., 1995. Understanding the Metropolis–Hastings algorithm. Am. Stat. 49, 327–335.

Clark, J.S., 2007. Models for Ecological Data: An Introduction. Princeton University Press, Princeton.

Cousens, N.B.F., Thomas, G.A., Swann, C.G., Healey, M.C., 1982. A review of salmon escapement estimation techniques. In: Can. Tech. Rep. Fish. Aquat. Sci. No. 1108.

de Valpine, P., Hastings, A., 2002. Fitting population models incorporating process noise and observation error. Ecol. Monogr. 72, 57–76.

Gauch, H.G., 2006. Winning the accuracy game. Am. Sci. 94, 133–144.

Gelman, A., Carlin, J.B., Stern, H., Rubin, D.B., 2004. Bayesian Data Analysis. Texts in Statistical Science. Chapman and Hall, London, UK.

Gelman, A., Hill, J., 2007. Data Analysis using Regression and Multilevel/Hierarchical Models. Cambridge University Press, New York.

Geweke, J., Tanizaki, H., 2001. Bayesian estimation of state-space models using the Metropolis–Hastings algorithm within Gibbs sampling. Comput. Stat. Data Anal. 37, 151–170.

Groot, G., Margolis, L., 1991. Pacific Salmon Life Histories. University of British Columbia Press, Vancouver.

Harwood, J., Stokes, K., 2003. Coping with uncertainty in ecological advice: lessons from fisheries. Trends Ecol. Evol. 18 (12), 617–622.

Harvey, A.C., 1989. Forecasting, Structural Time Series Models, and the Kalman Filter. Cambridge University Press, Cambridge, UK.

Hilborn, R., Walters, C.J., 1992. Quantitative Fisheries Stock Assessment and Management: Choice, Dynamics and Uncertainty. Chapman and Hall, New York.

Kehler, D.G., Myers, R.A., Field, C.A., 2002. Measurement error and bias in the maximum reproductive rate for the Ricker model. Can. J. Fish. Aquat. Sci. 59, 854–864.

Kope, R.G., 1988. Effects of initial conditions on Monte Carlo estimates of bias in estimating functional relationships. Can J. Fish. Aquat. Sci. 45, 185–187.

Korman, J., Peterman, R.M., Walters, C.J., 1995. Empirical and theoretical analyses of time-series bias in stock-recruitment relationships of Sockeye salmon (*Oncorhynchus nerka*). Can. J. Fish. Aquat. Sci. 52, 2174–2189.

Larkin, P.A., 1988. Pacific salmon. In: Gulland, J.A. (Ed.), Fish Population Dynamics: The Implications for Management. John Wiley and Sons, Chichester, pp. 153–183.

Ludwig, D., Walters, C.J., 1981. Measurement errors and uncertainty in parameter estimates for stock and recruitment. Can. J. Fish. Aquat. Sci. 38, 711–720.

Lunn, D.J., Thomas, A., Best, N., Spiegelhalter, D., 2000. WinBUGS—a Bayesian modelling framework: concepts, structure, and extensibility. Stat. Comput. 10, 325–337.

McGurk, M.D., 1986. Natural mortality of marine pelagic fish eggs and larvae: the role of spatial patchiness. Mar. Ecol. Prog. Ser. 34, 227–242.

Meyer, R., Millar, R.B., 2001. State-space models for stock-recruit time series. In: George, E.I. (Ed.), Bayesian Methods with Applications to Science, Policy, and Official Statistics; Selected Papers from ISBA 2000: The Sixth World Meeting of the International Society for Bayesian Analysis, Monograph in Official Statistics, Eurostat. , pp. 361–370.

Millar, R.B., 2002. Reference priors for Bayesian fisheries models. Can. J. Fish. Aquat. Sci. 59, 1492–1502.

Millar, R.B., Meyer, R., 2000. Non-linear state-space modeling of fisheries biomass dynamic using Metropolis–Hastings within Gibbs sampling. Appl. Stat. 49, 327–342.

Mueter, F.J., Peterman, R.M., Pyper, B.J., 2002. Opposite effects of ocean temperature on survival rates of 120 stocks of Pacific salmon (*Oncorhynchus* spp.) in northern and southern areas. Can. J. Fish. Aquat. Sci. 59, 456–463, plus the erratum printed in Can. J. Fish. Aquat. Sci. 60, 757.

Needle, C.L., 2001. Recruitment models: diagnosis and prognosis. Rev. Fish Biol. Fish. 11, 95–111.

Quinn, T.J., Deriso II, R.B., 1999. Quantitative Fish Dynamics. Oxford University Press, New York.

Peterman, R.M., Pyper, B.J., Grout, J.A., 2000. Comparison of parameter estimation methods for detecting climate-induced changes in productivity of Pacific salmon (*Oncorhynchus* spp.). Can. J. Fish. Aquat. Sci. 57, 181–191.

Petris, G., Petrone, S., Campagnoli, P., 2009. Dynamic Linear Models with R. Springer, New York.

Plummer, M., Best, N., Cowles, K., Vines, K., 2006. CODA: Convergence Diagnosis and Output Analysis for MCMC. R News 6, 7–11.

Pyper, B.J., Mueter, F.J., Peterman, R.M., 2005. Across-species comparisons of spatial scales of environmental effects on survival rates of Northeast Pacific salmon. Trans. Am. Fish. Soc. 134, 86–104.

Rivot, E., Prevost, E., Parent, E., 2001. How robust are Bayesian posterior inferences based on a Ricker model with regard to measurement errors and prior assumptions about parameters? Can. J. Fish. Aquat. Sci. 58, 2284–2297.

Rivot, E., Prevost, E., Parent, E., Bagliniere, J.L., 2004. A Bayesian state-space modeling framework for fitting a salmon stage-structured population model to multiple time series of field data. Ecol. Model. 179, 463–485.

Schnute, J.T., 1994. A general framework for developing sequential fisheries models. Can. J. Fish. Aquat. Sci. 51, 1676–1688.

Schnute, J.T., Kronlund, A., 2002. Estimating salmon stock-recruitment relationships from catch and escapement data. Can. J. Fish. Aquat. Sci. 59, 433–449.

Su, Z., Adkison, M.D., Van Alen, B.W., 2001. A hierarchical Bayesian model for estimating historical salmon escapement and escapement timing. Can. J. Fish. Aquat. Sci. 58, 1648–1662.

Su, Z., Adkison, M.D., 2002. Optimal in-season management of pink salmon given uncertain run sizes and seasonal changes in economic value. Can. J. Fish. Aquat. Sci. 59, 1648–1659.

Su, Z., Peterman, R., Haeseker, S., 2004. Spatial hierarchical Bayesian models for stock-recruitment analysis of pink salmon (*Oncorhynchus gorbuscha*). Can. J. Fish. Aquat. Sci. 61, 2471–2486.

Walters, C.J., 1985. Bias in the estimation of functional relationships from time series data. Can. J. Fish. Aquat. Sci. 45, 185–187.

Walters, C.J., 1990. A partial bias correction factor for stock-recruitment parameters in the presence of autocorrelated environmental effects. Can. J. Fish. Aquat. Sci. 47, 516–519.

Walters, C.J., Ludwig, D., 1981. Effects of measurement errors and uncertainty in parameter estimates for stock and recruitment. Can. J. Fish. Aquat. Sci. 38, 704–710.

Walters, C.J., Martell, S.J.D., 2004. Fisheries Ecology and Management. Princeton University Press, New Jersey.

Walters, C.J., Lichatowich, J.A., Peterman, R.M., Reynolds, J.D., 2008. Report of the Skeena Independent Science Review Panel. A report to the Canadian Department of Fisheries and Oceans and the British Columbia Ministry of the Environment , May 15, 2008, p. 144, available at: http://www.psf.ca/index.php?option=com_content&view=article&id=21&Itemid=49.